

# Synthesis and Characterization of Hydrophilic $\gamma$ -Fe<sub>2</sub>O<sub>3</sub> Nanoparticles for Biomedical Applications

TEODORA MALAERU\*, ELENA ENESCU, GABRIELA GEORGESCU, DELIA PATROI, EUGEN MANTA, EROS ALEXANDRU PATROI, CRISTIAN MORARI, VIRGIL MARINESCU

R&D National Institute for Electrical Engineering ICPE-CA Bucharest, 313 Splaiul Unirii, Bucharest, 030138, Bucharest, Romania

*The hydrophilic  $\gamma$ -Fe<sub>2</sub>O<sub>3</sub> nanoparticles coated with polyvinylpyrrolidone (PVP) were prepared in one step of the modified polyol method combined with an additional heat treating. The presence of maghemite ( $\gamma$ -Fe<sub>2</sub>O<sub>3</sub>) phase was confirmed by using X-ray diffraction (XRD) and Raman Spectrometry on powder. FT-IR spectroscopy confirmed the presence of PVP on the nanoparticles surface and the Zeta potential also supported the coating of nanoparticles with a layer of PVP and a good stability in aqueous medium. SEM analysis showed that the prepared  $\gamma$ -Fe<sub>2</sub>O<sub>3</sub> nanoparticles have a spherical structural morphology with the tendency of agglomeration. Hysteresis loop shows a ferromagnetic behaviour at room temperature with a saturation magnetization up to 57 emu/g.*

*Keywords:  $\gamma$ -Fe<sub>2</sub>O<sub>3</sub>, polyol method, magnetic nanoparticles, biomedical applications*

In the past decade, due to the physicochemical and their unique magnetic properties, iron oxide nanoparticles have been intensively studied by the scientific community for their scientific and technologic importance. They find applications in various fields, from magnetic recording [1] and environmental remediating [2] to biomedical applications such as magnetic resonance imaging (MRI) [3-5], treatment of cancer by hyperthermia [6, 7], separation of cells [8], drug delivery [9].

Among iron oxides, maghemite ( $\gamma$ -Fe<sub>2</sub>O<sub>3</sub>) is especially interesting for biomedical applications because it is non-toxic and presents both thermal and chemical stability. Also it has a chemically active surface where a variety of bonds allow the formation of biocompatible coatings. For biomedical applications magnetic nanoparticles need to be crystalline, non-agglomerated with optimized shape and size. By the synthesis process and controlling the process parameters, it is possible to control the resulting nanoparticles properties, such that nanoparticles with the same composition and crystalline structure have different chemical and magnetic properties. A wide variety of chemical synthesis methods has been reported in the literature for  $\gamma$ -Fe<sub>2</sub>O<sub>3</sub> nanoparticles preparation: coprecipitation [10, 11], microemulsion [12], sol-gel synthesis [13, 14], thermolysis [15], and thermal decomposition of iron complex [16]. Darezereshki E. reported the synthesis of  $\gamma$ -Fe<sub>2</sub>O<sub>3</sub> nanoparticles (size of 10 nm) obtained by coprecipitation of FeCl<sub>3</sub> and FeCl<sub>2</sub>•4H<sub>2</sub>O salts with NH<sub>4</sub>OH at pH = 9.73 and room temperature [17]. The monodispersed superparamagnetic  $\gamma$ -Fe<sub>2</sub>O<sub>3</sub> nanoparticles (15 - 20 nm) were prepared by a one-step thermal decomposition of iron (II) acetate in air at 400°C [18]. Monodisperse  $\gamma$ -Fe<sub>2</sub>O<sub>3</sub> nanoparticles with a diameter of particle of 13 nm were also prepared by the thermal decomposition of iron pentacarbonyl in presence of oleic acid at 100°C [16]. Via thermolysis of polyvinyl alcohol (PVA) gels, prepared under alkaline pH by adding Fe<sup>3+</sup> ions into warm aqueous solutions of PVA,  $\gamma$ -Fe<sub>2</sub>O<sub>3</sub> nanoparticles with diameters in the 7 - 18 nm range were synthesized [15].

For biomedical applications, is required that the iron oxide nanoparticles to be stable in water at neutral pH and

physiological salinity. Therefore, one of the main problems in producing stable iron oxide particles is to prevent their agglomeration during the synthesis and coating processes. For the surface modification of iron oxide particles with various biocompatible and biodegradable materials, the following approaches are presented in literature: organic vapour condensation, polymer coating, surfactant adsorption, and silanization using silane coupling agents [19]. In this study, hydrophilic  $\gamma$ -Fe<sub>2</sub>O<sub>3</sub> nanoparticles were prepared by a modified polyol method in the presence of ethylene glycol as solvent and poly-vinylpyrrolidone (PVP) reagent. The coating of nanoparticles with PVP has been realised in one step of the synthesis process. This modification of the surface of nanoparticles gives them water solubility and the biocompatibility required for biomedical applications.

## Experimental part

### Materials

Iron (III) Chloride Hexahydrate FeCl<sub>3</sub>•6H<sub>2</sub>O (≥ 98 %) purchased from FLUKA and Poly-vinylpyrrolidone (PVP) (M = 40000 g/mol) from SIGMA were used as reagents. Ethylene glycol (EG) (99%) purchased from CHIMOPAR was used as solvent and reducing agent, Sodium Acetate CH<sub>3</sub>COONa (99%) was used as a precipitating agent from REACTIVUL, Ethylic Alcohol Absolute C<sub>2</sub>H<sub>5</sub>OH (99.9 %) purchased from MERCK and Deionized Ultrapure Water, obtained from a Millipore Simplicity - UV equipment, were used at washing and purification.

### Synthesis of $\gamma$ -Fe<sub>2</sub>O<sub>3</sub> nanoparticles

In a 250 mL tree-neck round bottomed flask equipped with condenser, magnetic stirrer, thermometer and heating system was dissolved 4.05g (15 mmol) of FeCl<sub>3</sub>•6H<sub>2</sub>O in 150 mL of EG using magnetic stirring and heating to 100°C for 30 min. Then in the polyol-iron salt solution, 0.375g of PVP was added continuing magnetic stirring at 100°C for another 30 min. The thus obtained solution was gradually heated up to 200°C. In this moment 10.8 g of CH<sub>3</sub>COONa has been added, observing the formation of a precipitate of brown colour. The reaction mixture was maintained

\* email: teodora.malaeru@icpe-ca.ro, Phone: +40 21 3467231

under these conditions of reaction for 2h. The solution was then allowed to cool to room temperature and was centrifuged to remove traces of EG and PVP excess. Then the magnetically collected precipitate was washed five times with deionized water and with absolute ethylic alcohol at the end, and then it was dried at a temperature of 60°C in air for 4 h. The dried powder of the nanoparticles thus obtained and noted (S1), has been further heat treated at 270°C/1h and at 280°C/4h.

### Characterization

The powder of  $\gamma$ -Fe<sub>2</sub>O<sub>3</sub> nanoparticles was characterized by X-ray diffraction (XRD) analysis for the determination of the crystallographic structure, estimation of crystallite size and lattice parameter. The X-ray diffraction pattern of the powder samples was recorded on a D8 Discover, Bruker-AXS (Germany) diffractometer with CuK $\alpha$  (1.5406Å) at room temperature in the range of 10 to 100° in the 2 $\theta$  scale, with a scanning speed of 0.04°/s and a time step of 10s. Raman spectra were recorded using a Raman Spectrometer Model LabRAM HR Evolution, Horiba, using a 532 nm wave excitation and low power laser (about 0.1 mW). The spectra were acquired in the spectral range of 50-1700 cm<sup>-1</sup> at an acquisition time of 30 s x 10 accumulations/spectrum using a 600 g/mm diffraction network and a 50x ocular lens with a 0.75 numeric aperture. IR spectra were recorded with a Jasco 4200 spectrometer coupled with an attenuated total reflectance (ATR) module JASCO PRO 470-H ATR. The samples were measured directly by placing them on the crystal of the ATR and pressing with a controlled force, and the recording conditions of the spectra were as follows: spectral range: 4000 - 600 cm<sup>-1</sup>; resolution: 4 cm<sup>-1</sup>; number of scans/spectra: 50 accumulations. Thermal Analyses (TG/DTA) were performed on the powder sample with a heating rate of 10°C/min in the temperature range from room temperature up to 600°C by using a TG-DTA system (STA 490C, Netzsch-Germania).

The morphology and particle size of the as prepared samples were investigated by FESEM-FIB (Workstation Auriga) scanning electron microscope equipped with a dispersive X-ray spectroscopy (EDS) detector (Oxford Instruments). Chemical compositions were estimated by an area analysis using energy dispersive X-ray spectroscopy (EDS) system. The magnetic properties of the  $\gamma$ -Fe<sub>2</sub>O<sub>3</sub> samples were measured with a vibrating - sample magnetometer (VSM) Lake Shore 7300 model at room temperature. The prediction of the dispersion stability of the hydrophilic  $\gamma$ -Fe<sub>2</sub>O<sub>3</sub> nanoparticles in aqueous solution

was determined using NanoBrook ZetaPlus Zeta Potential Analyzer (Brookhaven, USA).

## Results and discussions

### Crystal structure analysis

The XRD pattern of the sample (S1) of  $\gamma$ -Fe<sub>2</sub>O<sub>3</sub> nanoparticles powder prepared by a modified polyol method was showed in figure 1.

As can be seen from the X-ray diffractogram of the sample (S1), the superposition of the peak positions for the  $\gamma$ -Fe<sub>2</sub>O<sub>3</sub> and Fe<sub>3</sub>O<sub>4</sub> could not confirm the phase of iron oxide nanoparticles. The X-ray diffractograms for the samples additionally heat treated presented in figure 2 (a) and (b), showed the formation of a single phase of the crystalline structure identified as being of the  $\gamma$ -Fe<sub>2</sub>O<sub>3</sub> according to the ICDD PDF (01-089-5892) catalogue sheet. The crystallite size was obtained using Debye-Scherrer equation (1) taking into account the main peak (311):

$$D = \frac{0.9\lambda}{B \cos\theta} \quad (1)$$

where: D is the crystallite mean size,  $\lambda = 1.5406\text{Å}$  is the wavelength of the X-rays, B is the full width at half maximum (FWHM) of the peak and  $\theta$  is the Bragg angle. The crystallite size of the as prepared samples determined in this manner are listed in table1.

The crystallite sizes increase with increasing temperature after applying additional thermal treatment from 8 nm to 10 nm (at 270°C/1h) and respectively 15 nm (at 280°C/4h).

In order to validate the crystalline structure of iron oxide, the samples were further analysed by Raman spectrometry. In figure 3 are shown the Raman spectra recorded on the samples S1 heat treated at 270°C/1h and at 280°C/4h respectively. One can notice the presence of an intense band with the maximum at approx. 689 cm<sup>-1</sup> which can be attributed to the presence of  $\gamma$ -Fe<sub>2</sub>O<sub>3</sub> in the analysed sample [20, 21]. As this temperature rises, this peak moves to the left and decreases in intensity. The low intensity peak at about 1400 cm<sup>-1</sup> also indicates the presence of  $\gamma$ -Fe<sub>2</sub>O<sub>3</sub> (22).

### FT-IR analysis

The Fourier Transform infrared (FT-IR) spectrum was used to characterize the surface chemistry and Fe-O bonds of the as synthesised  $\gamma$ -Fe<sub>2</sub>O<sub>3</sub> nanoparticles. The FTIR spectra obtained on the S1 heat treated sample at 270°C/1h (fig. 4) revealed the presence in the 490-700 cm<sup>-1</sup> region of a wide band with multi peak structure with maximum

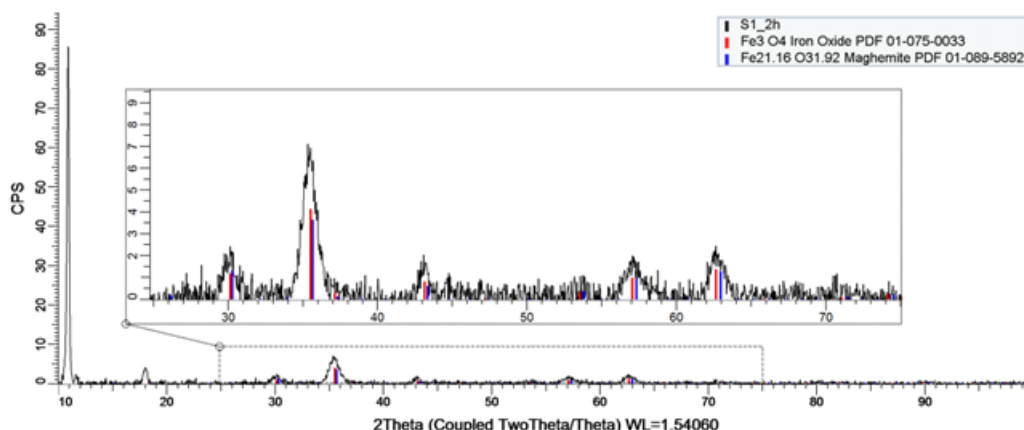


Fig. 1. X-ray powder diffraction patterns for (S1)  $\gamma$ -Fe<sub>2</sub>O<sub>3</sub> nanoparticles sample prepared by a modified polyol method

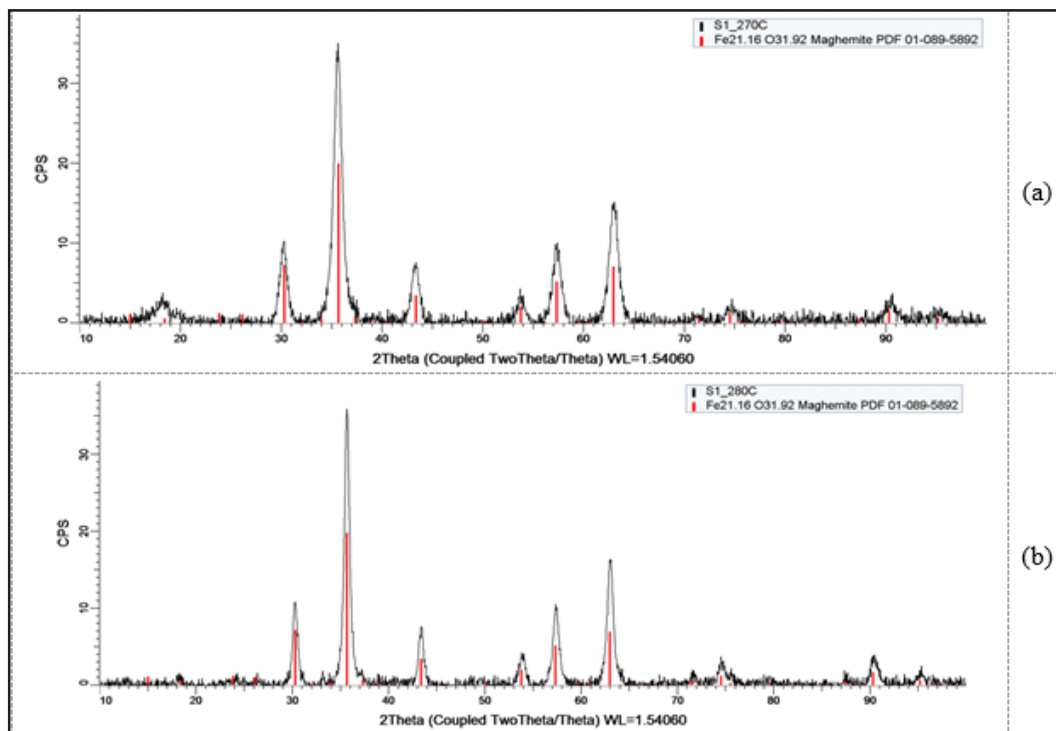


Fig. 2. X-ray powder diffraction patterns for (S1) $\gamma$ -Fe<sub>2</sub>O<sub>3</sub> nanoparticles sample prepared by a modified polyol method and subsequently heat treated to: (a) 270°C/1h and (b) 280°C/4h.

**Table 1**  
THE RESULTS OF XRD ANALYSIS FOR THE  $\gamma$ -Fe<sub>2</sub>O<sub>3</sub> NANOPARTICLES SAMPLES PREPARED

Sample	Crystalline phase	2 $\theta$ (degrees)	d (Å)	hkl	Lattice parameter		Crystallite size (nm)
					a <sub>teor</sub> (Å)	a <sub>exp</sub> (Å)	
S1	Fe <sub>3</sub> O <sub>4</sub> -centered cubic structure;	35.437	2.53106	311	8.3840	8.39457	8
	$\gamma$ -Fe <sub>2</sub> O <sub>3</sub> - cubic structure				8.3457		
S1 - 270 °C/1h	$\gamma$ -Fe <sub>2</sub> O <sub>3</sub> - cubic structure	35.609	2.5192	311	8.3457	8.3552	10
S1 - 280 °C/4h	$\gamma$ -Fe <sub>2</sub> O <sub>3</sub> - cubic structure	35.671	2.5150	311	8.3457	8.3413	15

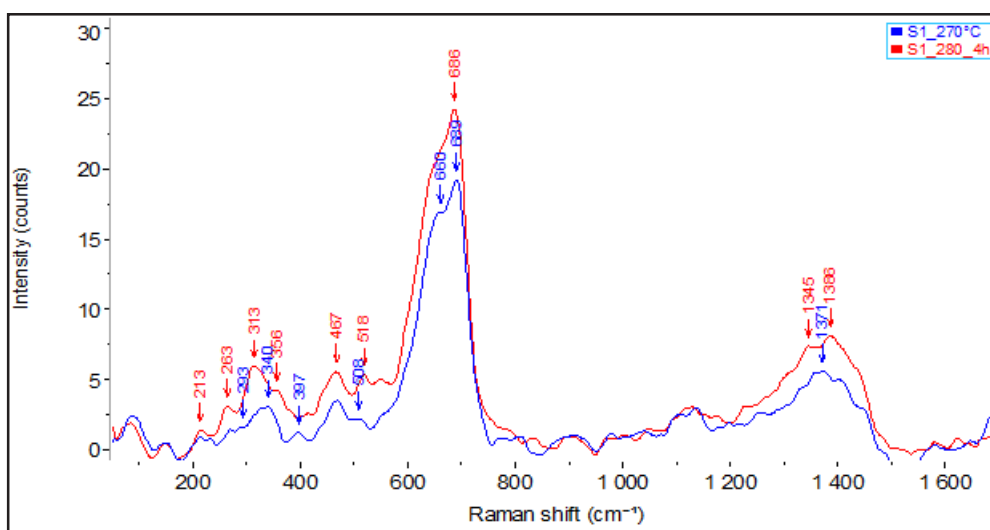


Fig. 3. The Raman spectrum recorded on sample S1 heat treated at 270°C/1h and at 280°C/4h.

values of approx. 672, 639, 570 and 546 cm<sup>-1</sup>, not very well defined. Also, the presence of bands (2820-2930 cm<sup>-1</sup>) attributed to vibration of the C-H bond and some bands at 1720 cm<sup>-1</sup> attributed to vibration of the C = O bond, was observed. They support surface coating of the  $\gamma$ -Fe<sub>2</sub>O<sub>3</sub> nanoparticles with PVP.

#### Thermal analysis

Figure 5 shows the TG-DTA curves of the sample S1 synthesized by the modified polyol method before the application of an additional thermal treatment.

The TG curve of the sample S1 in the analysed temperature range is characterized by a gradually mass loss. At approx. 160°C there is a loss of approx. 3% without

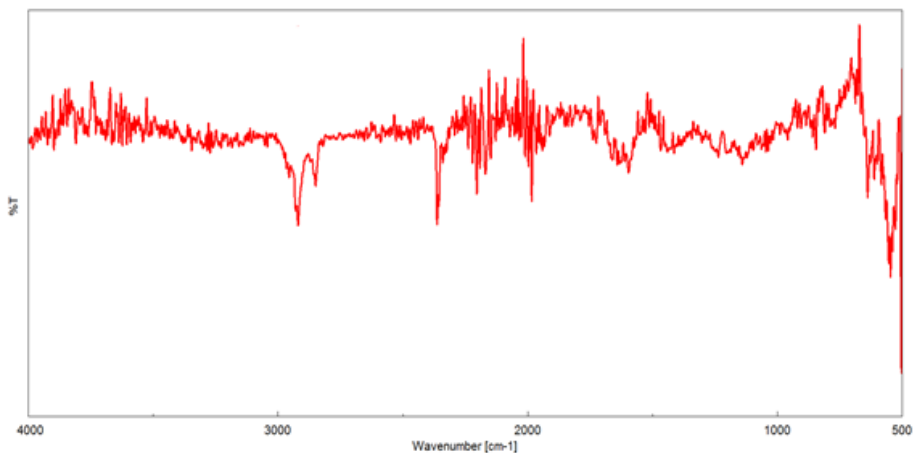


Fig. 4. The FTIR spectrum recorded on S1 sample heat treated to 280°C/4h.

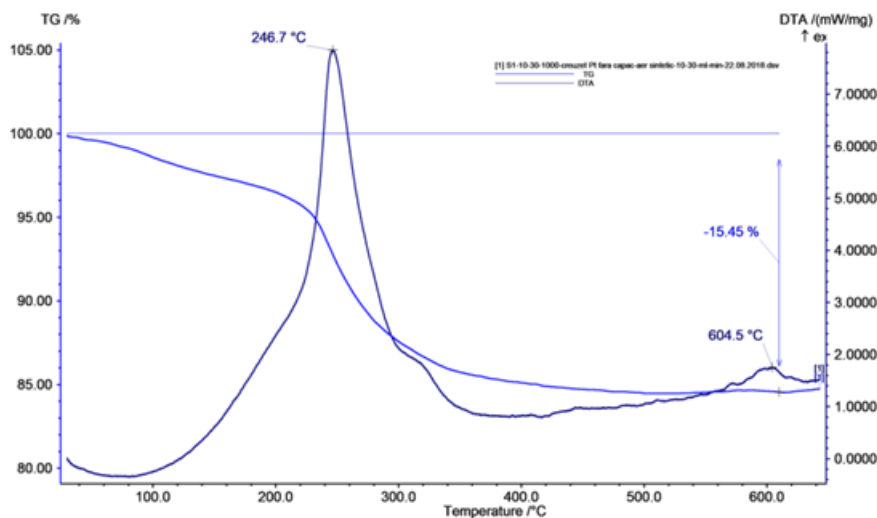


Fig. 5. The TG-DTA curves of iron oxide nanoparticles (sample S1) synthesized by the modified polyol method before applying an additional thermal treatment.

a visible thermal effect and in the intervals of 200-300 and 300-500°C there is a mass loss of 14.50-15.45% associated with a pronounced exothermic effect which is likely due to the thermal decomposition and the burning of the sample with a large heat release of 6.4 mW/mg. In the range of 400-580°C the mass is constant - no thermal effects arise which shows that at a temperature above 300°C a stable oxide system -  $\gamma$ -Fe<sub>2</sub>O<sub>3</sub> has been formed. On the DTA curve, there is a small exothermic effect at 604.5°C without loss

of mass that may be due to redistributions in the previously formed oxide network at approx. 300°C.

#### EDS-analysis

The energy dispersive spectrometer (EDS) was used to analyse the chemical composition of the sample. The EDS pattern of the as synthesized  $\gamma$ -Fe<sub>2</sub>O<sub>3</sub> nanoparticles (fig. 6) showed the presence of Fe, O and C elements. The presence of element C suggests that the nanoparticles

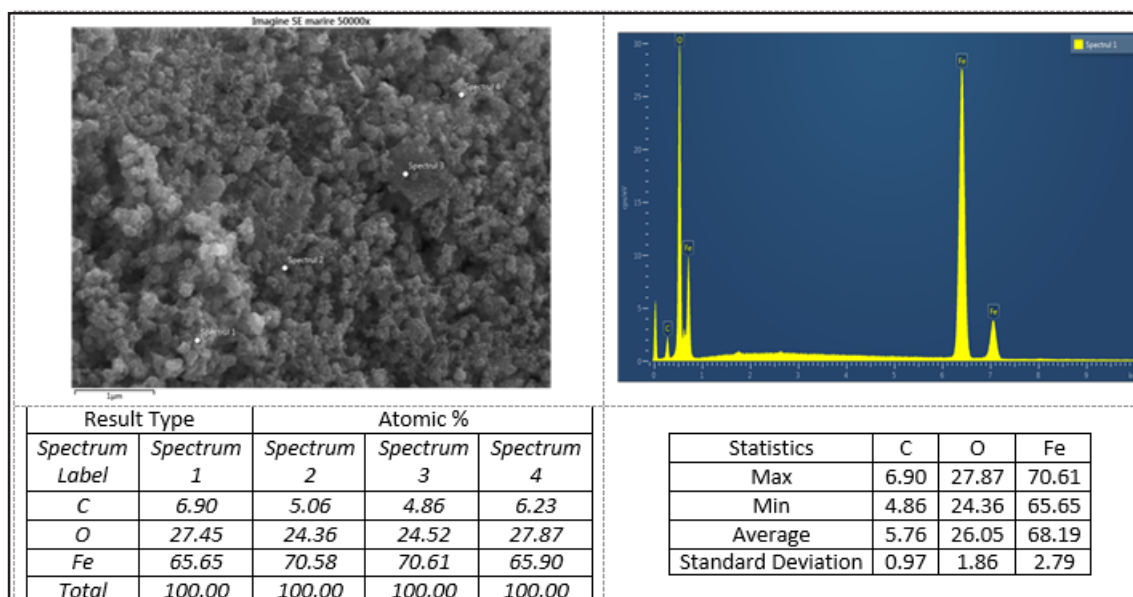


Fig. 6. The EDS pattern of the  $\gamma$ -Fe<sub>2</sub>O<sub>3</sub> nanoparticles prepared by a modified polyol method and subsequently heat treated to 270°C/1h.

were covered with the organic PVP layer. Also, EDS analysis was able to estimate the elements concentration (70.61% Fe, 27.87% O and respectively 6.9% C). While considering the atomic weights of iron and oxygen as 55.85 and 16, the weight ratio of iron and oxygen concentrations in the sample was estimated and the ratio of elements came close to the empirical formula of  $\text{Fe}_2\text{O}_3$ . This confirms that the nanoparticles obtained are  $\gamma\text{-Fe}_2\text{O}_3$  and not magnetite ( $\text{Fe}_3\text{O}_4$ ).

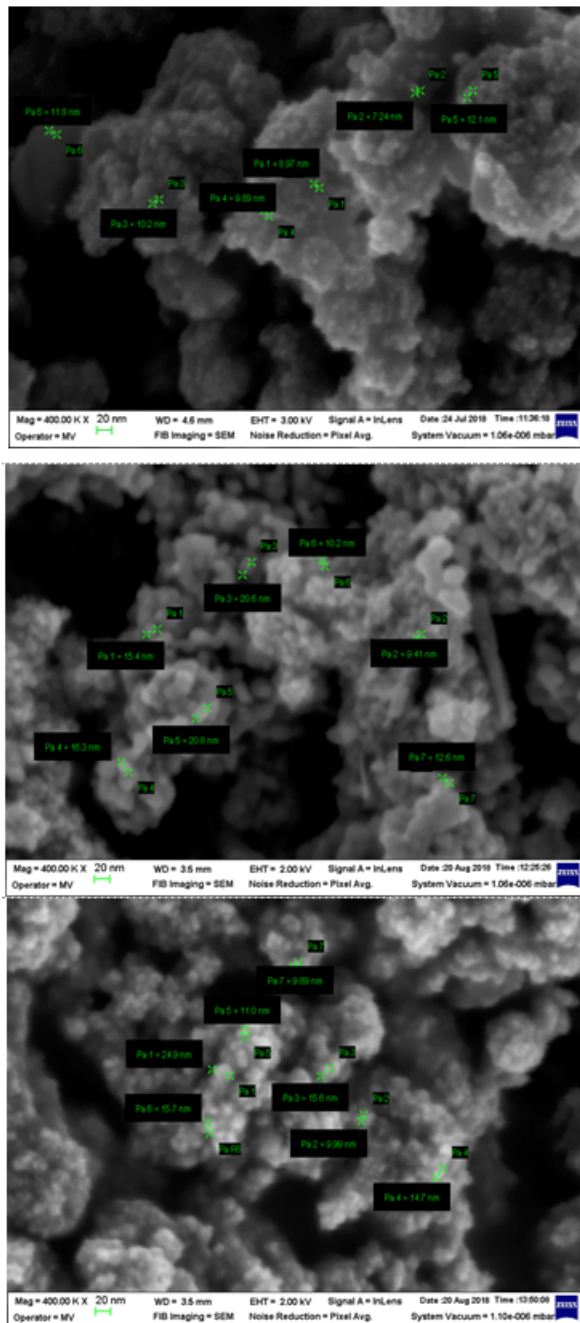


Fig. 7. The SEM images of the  $\gamma\text{-Fe}_2\text{O}_3$  nanoparticles prepared by a modified polyol method (a) and subsequently heat treated to (b)  $270^\circ\text{C}/1\text{h}$  and to (c)  $280^\circ\text{C}/4\text{h}$ .

Sample	Remanent magnetization ( $M_r$ ) [emu/g]	Saturation magnetization ( $M_s$ ) [emu/g]	Coercivity field ( $H_c$ ) [A/m]/[Oe]
S1	6	25	19679.64/ 247
S1 - 270 $^\circ\text{C}/1\text{h}$	15	52	19974.07/ 251
S1 - 280 $^\circ\text{C}/4\text{h}$	20	56	24852.21 / 312

### SEM analysis

The SEM images of the synthesized  $\gamma\text{-Fe}_2\text{O}_3$  nanoparticles powder are presented in figure 7 (a) - (c).

The morphology of the as prepared  $\gamma\text{-Fe}_2\text{O}_3$  nanoparticles showed an approximate spherical shape with the tendency of agglomeration. The particles size resulting from the SEM analysis was coincident with the XRD analysis.

### VSM analysis

Figure 8 shows the magnetization vs. magnetic field loops measured at room temperature for the samples of  $\gamma\text{-Fe}_2\text{O}_3$  nanoparticles prepared. Hysteresis loops show that all the nanoparticles have ferromagnetic behaviour at room temperature.

Table 2 shows the magnetic parameters of the  $\gamma\text{-Fe}_2\text{O}_3$  nanoparticles samples. The saturation magnetization ( $M_s = 25.45$  emu/g) value for the  $\gamma\text{-Fe}_2\text{O}_3$  nanoparticles (sample S1) is significantly lower than those of heat treated samples due to the indefinite crystalline structure of iron oxide. With increasing of heat treatment temperature, the saturation magnetization value increases from 51.59 emu/g for sample S1 treated at  $270^\circ\text{C}/1\text{h}$  to 55.56 emu/g for sample S1 treated at  $280^\circ\text{C}/4\text{h}$ . However, the saturation magnetization values are lower than those of the bulk  $\gamma\text{-Fe}_2\text{O}_3$  (76 emu/g) [24, 25] due to the presence of the nonmagnetic (PVP) coating and the small size effect of the  $\gamma\text{-Fe}_2\text{O}_3$  particles.

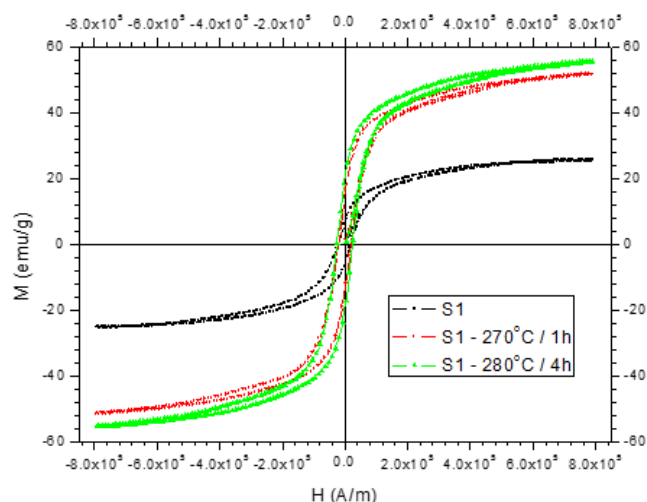


Fig. 8. M vs. H hysteresis loops for the as prepared  $\gamma\text{-Fe}_2\text{O}_3$  nanoparticles samples.

### Zeta potential analysis

Figure 9 shows the Zeta potential recorded on an aqueous solution (0.01%) of the  $\gamma\text{-Fe}_2\text{O}_3$  nanoparticles prepared by the modified polyol method combined with

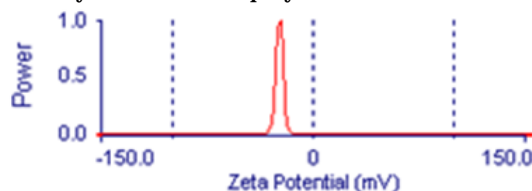


Fig. 9. Zeta Potential of the  $\gamma\text{-Fe}_2\text{O}_3$  nanoparticles prepared by a modified polyol method and subsequently heat treated to  $280^\circ\text{C}/4\text{h}$

**Table 2**  
MAGNETIC PARAMETERS OF THE  $\gamma\text{-Fe}_2\text{O}_3$   
NANOPARTICLES SAMPLES

an additional thermal treatment at 280°C/4h at a pH of 7.5. The value of the resulting Zeta potential of -28 mV indicates good aqueous medium stability of the  $\gamma$ -Fe<sub>2</sub>O<sub>3</sub> nanoparticles thus prepared, supporting the surface modification of nanoparticles by coating with a fine layer of PVP hydrophilic polymer.

## Conclusions

The hydrophilic  $\gamma$ -Fe<sub>2</sub>O<sub>3</sub> nanoparticles were successfully prepared in one step of the modified polyol method in the presence of PVP and with additional thermal treating at 270°C/1h and at 280°C/4h. Raman spectrometry confirmed the presence of the  $\gamma$ -Fe<sub>2</sub>O<sub>3</sub> unique phase. Increasing temperatures and heat treatment time led to increasing the degree of crystallinity and crystalline sizes from 10 to 15 nm without affecting the structural composition. The presence of the PVP layer on the surface of prepared  $\gamma$ -Fe<sub>2</sub>O<sub>3</sub> nanoparticles was confirmed by the results of FT-IR, EDS analyses and by the water dispersibility stability (zeta potential). The result of VSM analysis revealed ferromagnetic behaviour at room temperature. The Ms value increases with the increase in crystallinity and particle sizes reaching a value of 56 emu/g for the S1 sample thermally treated at 280°C/4h. The magnetic properties and good stability in the aqueous medium were encouraging for using PVP-coated  $\gamma$ -Fe<sub>2</sub>O<sub>3</sub> nanoparticles prepared by polyol method in biomedical application.

*Acknowledgement: This work was supported by project PN no.18240101/2018 and project no.30 PFE/2018 between National R&D Institute for Electrical Engineering ICPE-CA and Romanian Ministry of Research and Innovation (MCI).*

## References

1. ZENG, S.Y., TANG, K.B., LI, T.W., J. Colloid. Interface Sci., **312**, 2007, p. 513.
2. SHALINI, R., CHARLES, U., PITTMAN Jr., DINISH, M., J. Colloid. Interface Sci., **468**, 2016, p. 334.
3. BULTE, J.W., Methods Mol. Med., **124**, 2006, p.419.
4. LI, L., JIANG, W., LUO, K., SONG, H., LAN, F., WU, Y., GU, Z., Theranostics, **3**, no.8, 2013, p.595.
5. BARBARA, B., FRANK, C.J.M., VEGGEL, B.T., J. Nanomater., **2013**, 2013, p.1.

6. HERGT, R., HIERGUST, R., HILGER, I., KAISER, W.A., LAPATNIKOV, S., MARGEL, S., RICHTER, U., J. Magn. Magn. Mater., **270**, no.3, 2004, p. 345.
7. COVALIU, C.I., GEORGESCU, G., JIATARU, I., NEAMTU, J., MALAERU, T., OPREA, O., PATROI, E., Rev. Chim. (Bucharest), **60**, no. 12, 2009, p.1254.
8. BUCAK, S., JONES, D.A., LAIBINIS, P.E., HATTON, T.A., Biotechnol. Prog., **19**, 2003, p.477.
9. KARAMPOUR, S., SADJADI, M.S., FARHADYAR, N., Spectrochimica Acta-Part A: Molecular and Biomolecular Spectroscopy, **148**, 2015, p.146.
10. JEONG, J.R., LEE, S.J., KIM, J.D., SHIN, S.C., Phys. Status Solidi B, **241**, 2004, p.1593.
11. GOZDE, U., UFUK, G., OPREA, O., FICAI, D., SONMEZ, M., RADULESCU, M., ALEXIE, M., FICAI, A., Curr. Top. Med. Chem., **15**, 2015, p. 1.
12. TUEROS, M.J., BAUM, L.A., BORZI, R.A., STEWART, S.J., MARCHETTI, S.G., BENGGOA, J.E., MOGNI, L.V., Hyperfine Interact., **148-149**, 2003, p.103.
13. TAO, S.W., LIU, X.Q., CHU, X.F., SHEN, Y.S., Sensor Actuat. B-Chem., **61**, 1991, p.33.
14. ZHANG, L., PAPAFTYMIOU, G.C., YING, J.Y., J. Appl. Phys., **81**, 1997, p. 6892.
15. RUHUL, A.B., PALASH, B., BIRINCHI, K. Das, Journal of Saudi Chemical Society, **21**, 2017, p. S170.
16. TAEGHWAN, H., SU, S.L., JONGNAM, P., YUNHEE, C., HYON Bin Na, J. Am. Chem. Soc., **123**, 2001, p. 12798.
17. DAREZERESHKI, E., Mater. Lett., **64**, 2010, p. 1471.
18. KLUCHOVA, K., ZBORIL, R., TUCEK, J., PECOVA, M., ZAJONCOVA, I., JANCIK, D., SEBELA, M., BARTONKOVA, H., BELLESI, V., NOVAK, P., PETRIDIS, D., Biomaterials, **30**, 2009, p. 2855.
19. YONIT, B., SHLOMO, M., J. Colloid. Interf. Sci., **317**, 2008, p. 101.
20. SLAVOV, L., ABRASHEV, M.V., MERODIJSKA, T., CELEV, Ch., VANDENBERGHE, R.E., MARKOVA-DENEVA, I.N., J. Magn. Magn. Mater., **322**, no.14, 2010, p.1904.
21. HANESCA, M., Geophys. J. Int., **177**, 2009, p. 941.
22. RUBIM, J.C., SOUSA, M.H., SILVA, J.C.O., TOURINO, F.A., Braz. J. Phys., **31**, no.3, 2001, p. 402.
23. CORNELL, R.M., SCHWERTMANN, U., in Iron Oxides 2nd ed., 2003, p. 146.
24. LIU, Z.L., LIU, Y.J., YAO, K.L., DING, Z.H., TAO, J., WANG, X., J. Mater. Synth., Process, **10**, 2002, p. 83
25. MALAERU, T., PATROI, E.A., MARINESCU, V., OPREA, O., PATROI, D., MORARI, C., MANTA, E., GEORGESCU, G., Rev. Chim. (Bucharest), **70**, no. 2, 2019, p. 459.

Manuscript received: 6.12.2018